

Christian Janot
Institut Laue-Langevin
Grenoble, France

Abstract

Quasicrystals are a new form of solid state which differ from both crystal and amorphous compounds by possessing a new type of long-range translational order, quasiperiodicity, and a noncrystallographic orientational order. Several geometrical schemes can be used to describe quasiperiodic structures, including cut and projection from an hyperspace periodic structure, space tiling with matching rules, selfsimilar packing of clusters or even simplistic growth procedure within some constraints.

Introduction

Quasicrystals are materials having a new type of long range order such that their diffraction patterns show Bragg reflections revealing symmetries which are incompatible with periodicity [1]. However, they are highly ordered systems [2] with correlation length of several tenths of a micrometer [3]. Large single (quasi)crystals have been grown [4] whose structural quality is such that dynamical diffraction has been observed [3]. Deciphering the atomic structure of quasicrystals via classical techniques of crystallography has been reasonably well achieved using the relation of a quasiperiodic function with its hyperspace periodic image [5], even if details about atom positions are still missing.

Aside from their peculiar structures, quasicrystals also exhibit very unexpected properties [6]. Their perhaps most intriguing feature is a very high electrical (and thermal as well) resistivity. Its value which is almost as large as that of insulators [7] is amazing indeed for a material containing about 70% of aluminium. Reduced surface wetting, low friction, high hardness, weak chemical reactivity are among other interesting properties of quasicrystals. It is a current consensus that such physico-chemical behaviours are rooted somewhere into the still unusual geometry of these structures.

Substitution rules for growing quasicrystals

Making a structure grow is always a tiling story: polyhedra are first selected, then decorated with atoms of one or several chemical species and finally the structure results from packing copies of these decorated polyhedra. The packing obtained is a tiling of the space if there are neither holes nor overlaps of polyhedra in the built structure. The classical (periodic) crystals, based on the observation of natural minerals, deals with the simplest tiling procedure you can think of: a single type of tile is added again and again by translation. But addition is not the only way to fill space in good order. Iterative substitution rules offer an interesting alternative. To illustrate the difference between geometrical addition (*GA*) and geometrical substitution (*GS*), consider linear (one-dimensional) chains built up with sequences of two segments one large (*L*) and one short (*S*). *GA* structures can be obtained by adding strips *LS* over and over again, resulting in the periodic chain *LSLSLSLS...* To obtain a *GS* chain, substitution rules must be used instead. There is of course an infinite variety of substitution rules. For instance, any given strip of *L*, *S* segments can be grown by substituting *L* by *LS* and *S* by *L* iteratively; this results in the following successive grown strips:

- initial strip: *LS*
- first substitution: *LSL*
- second substitution: *LSLLS*
- third substitution: *LSLLSLSL*
- fourth substitution: *LSLLSLSLLSLLS*
- etc.

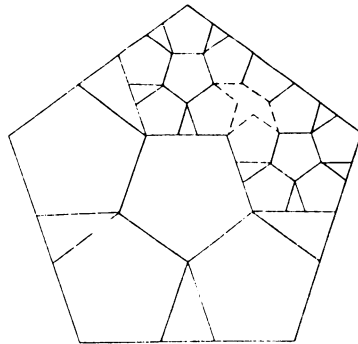


Figure 1: Substitution rules for planar tiling with a pentagonal symmetry.

The final chain is a perfectly ordered, deterministic sequence of L and S segments without any indication of periodicity. It is easy to see that the strip S_n obtained after n iterative steps is the simple addition of the strips S_{n-1} and S_{n-2} obtained after $n - 1$ and $n - 2$ steps respectively. Self similarity of the grown structure is then obvious.

Some other properties of the above quasiperiodic chain (Fibonacci chain) are of interest, inasmuch as they are easily generalised to two and three dimensional quasiperiodic structures.

First of all, let us count the number of L and S segments in the chain strips obtained after each substitution step.

This gives:

- start situation: one L , one S
- after one step: two L , one S
- after two steps: three L , two S
- after three steps: five L , three S
- after four steps: eight L , five S
- etc.

The number of $L(S)$ segments after n steps of substitution is equal to the sum of $L(S)$ segments found after $n - 1$ and $n - 2$ steps. The ratio of L segment numbers over S segment numbers takes successively, according to substitution steps, the values $1/1, 2/1, 3/2, 5/3, 8/5, 13/8$, etc. This is precisely the Fibonacci series whose limit is the golden mean $\tau = (1 + \sqrt{5})/2 = 2 \cos 36^\circ$ when the chain is grown ad infinitum.

The substitution rule as applied in the present case forces also the length ratio L/S to be equal to τ , indeed:

$$x = \frac{L}{S} = \frac{L + S}{L}$$

or: $x^2 = x + 1$ with $x > 1$

which has the single mathematical solution $x = \tau$. Consequences will be that a quasicrystal must be made of at least two different chemical species mixed in strictly defined proportions and occupying well defined partial volumes. A growth rule may also be deduced in which density fluctuation would be bounded via the requisite that the numbers of L and S segment remain in a ratio close to τ .

Differences in properties for periodic GA and aperiodic GS chains can be easily anticipated. For instance, in a monatomic GA chain, such as a metal

crystal, all atomic sites are strictly equivalent. If some electrons are loosely bonded to atoms they have no reason to locate on a particular site and can travel essentially freely through the bulk of the metal. This results in high conductivity and isotropy of the properties. Conversely, in *GS* structures strictly equivalent sites cannot be found if the fully extended surroundings of the sites is considered. The “free” electrons, if any, are forced to “locate” recurrently into hierarchies of sites according to an energy scale and within the constraints of Coulomb interactions. Actually, quasiperiodic structure, are such that identical site domains of any size can be found recurrently at distances apart of about twice the domain size. This is easily checked with the Fibonacci chain, if not too small domains are considered. Thus, delocalization via hopping between domains of a given class of local isomorphism can be reasonably expected.

For one-dimensional structures, it may be difficult to imagine why this awkward substitutional operation should be preferred instead of straightforward periodic packing. But in two and three dimensions, the latter may be just impossible. This is the situation, for instance, with pentagonal or icosahedral tiles whose fivefold symmetries cannot be accommodated by periodicity. Consequently aperiodic structures become the stable solution when chemical bonding favours such local “non-crystallographic” symmetries. This has been demonstrated by both numerical simulations [8] and experimental observations [5, 9].

Aperiodic tiling of the two-dimensional space

The substitutional growth is formally extended to two- and three-dimensional tiling without basic difficulties. This is illustrated in Figure 1 which shows how to grow a pentagonal tiling. Starting with a pentagonal area, six second generation pentagons and five triangles share the available space. Applying the same substitutional rules to the second generation pentagons introduces an additional “boat shape”, as it is shown in Figure 2. In this particular example, R. Penrose [10] has proved that four and only four prototiles are needed to pursue the tiling ad infinitum: a pentagon, a triangle, a “boat shape”, and a fivefold star. More precisely, holes which may form while growing the structure can always be filled in by one to these four tiles of the same generation. Simple geometrical derivations give the linear and surface deflation factors of the above procedure: τ^2 and τ^4 respectively. By multiplying the tiling size by these factors after each substitutional operation one get a growing tiling made of constant size elementary tiles.

Finally, it is worth pointing out that a simulated diffraction pattern with atoms sited on the vertices of such a tiling reproduces qualitatively experimental data (Figure 3) and clearly shows long range order and fivefold symmetries.

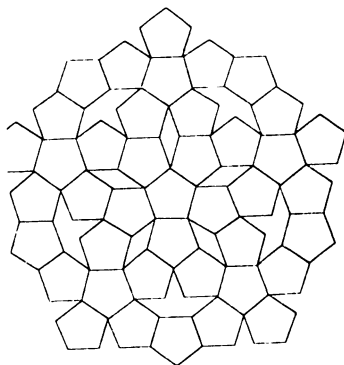


Figure 2: Further growth of the pentagonal tiling.

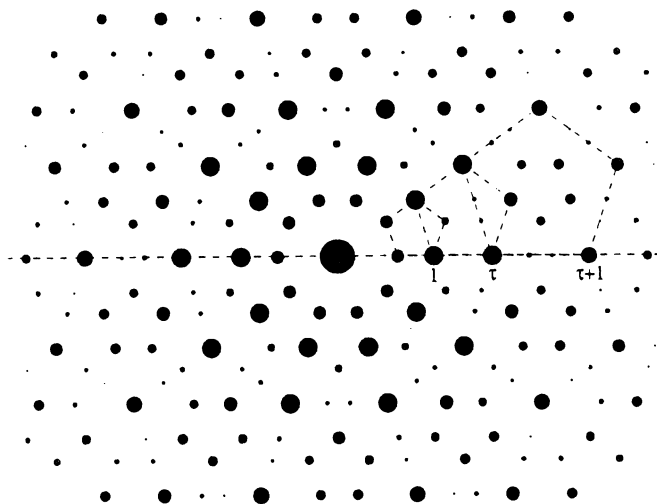


Figure 3: Numerical simulation of a diffraction pattern for the pentagonal tiling shown in Figure 2.

Again R. Penrose [10] has demonstrated that, in the case of most of the two-dimensional quasiperiodic tilings, the number of prototiles can be reduced to two. One example is given in Figure 4 for a fivefold tiling based on two triangles prototiles A and B with master angles $\pi/5$ and $2\pi/5$ respectively and area ratio equal to τ . The substitutional operation used to grow the structure is

also illustrated in Figure 4 ($A_n = A_{n-1}B_{n-1}A_{n-1}$ and $B_n = A_{n-1}B_{n-1}$). It is very easy to verify that the sizes expand as $B_{n+1} = \tau^2 B_n$ and $A_{n+1} = \tau^2 A_n$. The grown structure is selfsimilar but not fractal ($d_f = 2$). Again the number of prototiles A divided by the number of prototiles B in the growing tiling is a figure which follows the Fibonacci series and has a limit equal to τ when the tiling is grown ad infinitum.

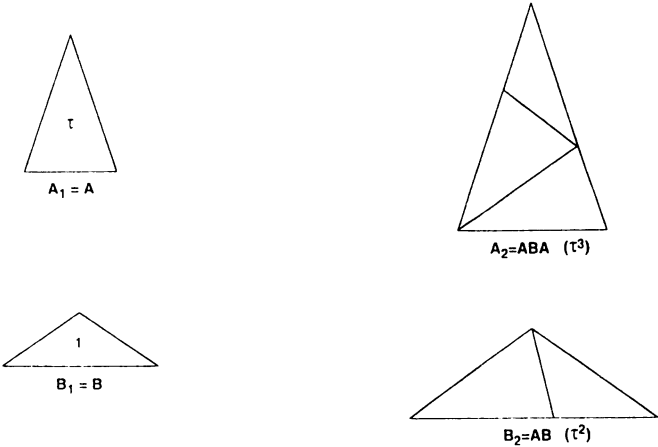


Figure 4: Triangular tiles and substitution rules for an alternative fivefold tiling of the plane.

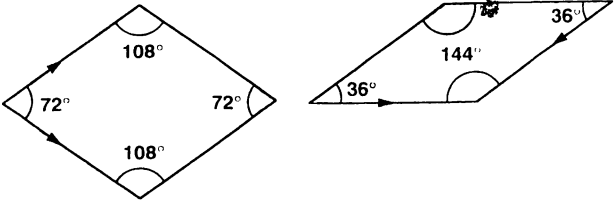


Figure 5: Rhombic prototiles with matching rules for the Penrose tiling.

The most famous modification of the fivefold two dimensional tiling is the so-called Penrose tiling which is based on two rhombic prototiles as shows in Figure 5, along with proper decorations which define matching rules in a growth

procedure: when a tile is added, full dark or full white circles must be completed at the vertices, excluding mixed dark and white circles, and arrows on edges must match identically. Penrose tilings have fascinating properties. Despite being aperiodic, similar domains repeat in the structure over and over again, as clearly visible in Figure 6 (see for instance the "star" made of five "fat" rhombic units). One can also verify directly on Figure 6 that any type of domain, of any size, is reproduced ad infinitum at distances apart twice their size. Iterative substitution and matching rules are equivalent procedures to grow aperiodic structures (Fig. 7). A more tricky geometrical feature can be observed by looking carefully at Penrose tiling schemes: actually an infinite number of slightly different Penrose tilings can be obtained within proper respect of given matching rules; these various modifications cannot be globally superimposed to each other but, amazingly, any area selected in one of the tiling is also found in the other parent tilings. This curiosity is going to be explained via the cut/projection scheme later on in the paper.

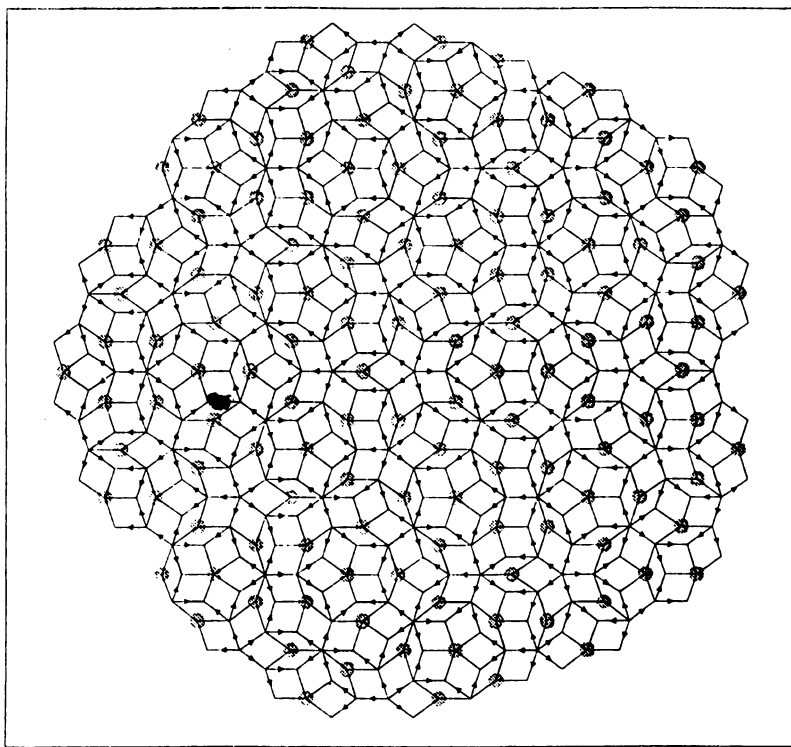


Figure 6: Piece of Penrose tiling as obtained with the prototiles and matching rules shown in Figure 5.

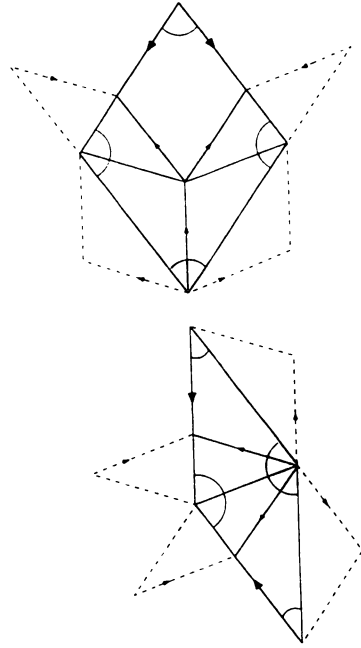


Figure 7: Iterative substitution rules for growing a Penrose tiling via self similar inflation.

The geometrical ingredient leading to Penrose tiling can be easily extended to planar tilings of any symmetries, except for two-, three-, four- and six fold rotations which allow periodic tilings. The example of a thirteen-fold tiling is shown in Figure 8.

Even the simplest iterative substitution rules seems to require more than one prototile to grow a planar quasiperiodic structure. But this has not been rigorously proved. On the other hand, one may accept to forget tiles and tiling and use motives instead. Conversely to a tile which is a bulky geometrical shape refusing overlaps, a motive is made of dots and can overlap. In the Penrose tiling of Figure 6, decagonal overlapping motives are clearly visible [11]. It has been suggested that such overlapping motives or equivalently, atomic clusters, are the pertinent basic units in the growth scheme of real quasicrystals [8, 12]. This is going to be advocated further in a forthcoming section of the paper.

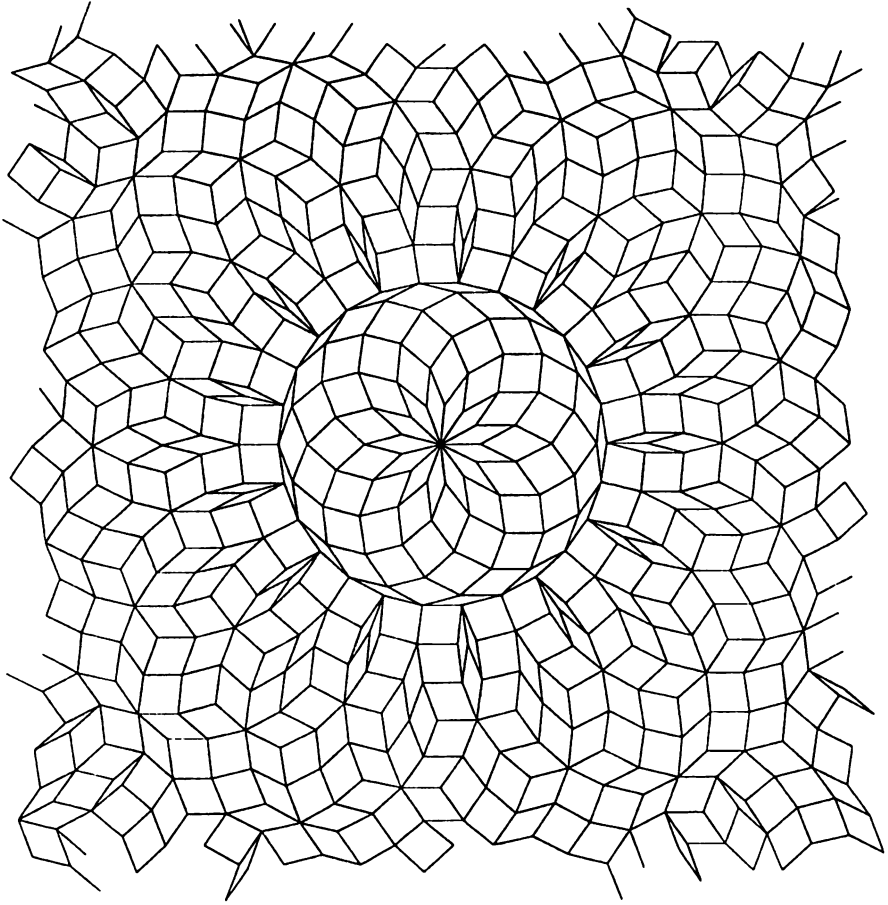


Figure 8: Example of a thirteen-fold planar tiling.

The three-dimensional situation

It is obviously possible to consider any aperiodic planar tiling of the sort described previously and to pile up them periodically in a direction perpendicular to the tiling plane. Real quasicrystals have indeed been obtained with such uniaxial symmetries but only five, eight, ten and twelve-fold rotations have been actually observed. Amusingly enough, the corresponding polygones are those which can be most easily drawn with only a ruler and a pair of compasses!

Now, if the three-dimensional space is to be tiled quasiperiodically in all directions, one must combine several rotations in such a way that the images of

any point remains on a finite trajectory, inside a polyhedron which then can be used as a prototile. For instance, using the symmetry operations of a cube gives trajectories of 48 points. All other geometrical possibilities have been known for quite a long time. They include the 32 rotation groups which give rise to periodic crystal structures. Beyond them, there are only two more cases which correspond to symmetries of an icosahedral polyhedron: either the 60 rotations or 120 operations by adding mirror planes to the rotations. Fully three-dimensional quasicrystals can then be only of the icosahedral species. This is actually well consistent with physical reality.

Formal extension of the 2-dimensional Penrose tiling is straightforward. Instead of planar rhombic units, bulky rhombohedral tiles are used: they are designed in either an oblate or a prolate shape; all edges are equal; angles of their rhombic faces are 63.43° or 116.57° , precisely those found in between fivefold axes of an icosahedron. Assembling these rhombohedra to generate a 3-dimensional quasiperiodic order requires to select proper matching rules in the form of appropriate decoration of faces and vertices. The practical building of such a tiling suffers actual difficulties which make the procedure both effectively intractable and physically implausible. The hyperspace scheme offers a more acceptable alternative.

The periodic image of quasicrystals

Both crystal and quasicrystal structures can be analysed in terms of their Fourier components in that the space dependence of the density can be expressed as a sum of density waves, i.e:

$$\rho(r) = \frac{1}{V} \sum_G F(G) \exp(iG \cdot r) \quad (1)$$

For periodic crystals, the sum (1) is zero except for those G vectors which define a discrete reciprocal periodic lattice and can then be written as an integer linear combination of three basis vectors a_i^* , i.e:

$$G = ha_1^* + ka_2^* + la_3^* \quad (2)$$

in which the integers h, k, l , are the so-called Miller indices for the structure factor $F(G)$ appearing in Eq. (1).

The diffraction pattern of a quasicrystal, as the one shown in Figure 9, cannot obviously be interpreted with a lattice of G vector given by Eq. (2). But a careful

investigation of the pattern suggests that actually only a few things must be modified. The density wave description by Eq. (1) is still valid; the G vectors still form a discrete set but Eq. (2) must be modified into:

$$G = n_1 a_1^* + n_2 a_2^* + n_3 a_3^* + n_4 a_4^* + n_5 a_5^* + n_6 a_6^* \quad (3)$$

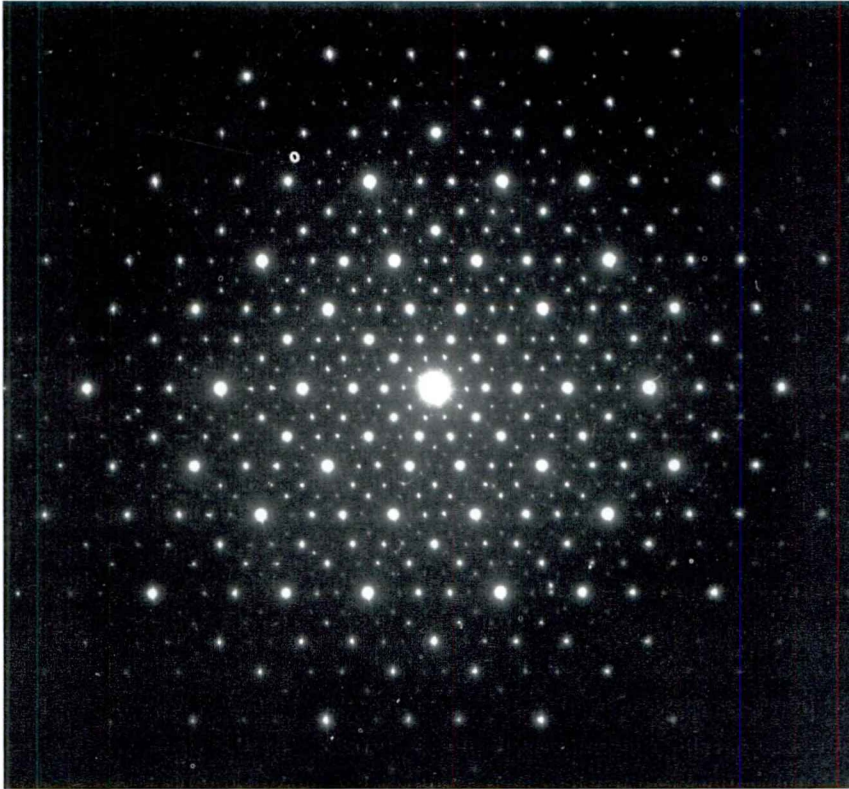


Figure 9: Electron diffraction pattern of an icosahedral quasicrystal of the AlFeCu system.

in which the n_i are integers and the a_i^* vectors are lying along the six fivefold axes of an icosahedron (Fig. 10). These a_i^* 's cannot be reduced to three members via any projection scheme on reference axes; the resulting "Miller indices" would be always fractional numbers due to irrationality of the cosine and sine functions for the angles between a_i^* 's ($63^\circ 43'$ or $116^\circ 57'$). Using the reference axes of the Figure 10, Eq. (3) can be given a equivalent expression in the form of three

orthogonal components for the G vectors, i.e.:

$$G \begin{cases} h + \tau h' \\ k + \tau k' \\ l + \tau l' \end{cases} \quad (4)$$

(h, h', k, k', l, l' are integers and τ is the golden mean).

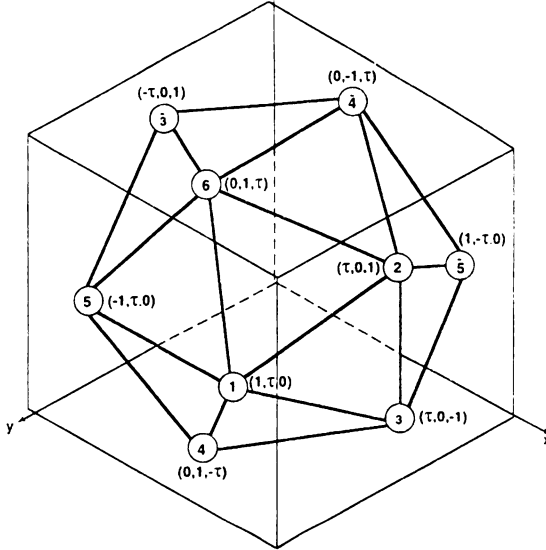


Figure 10: Icosahedron showing the fivefold axis vectors a_i^* with their components in an orthogonal frame:

$$\begin{array}{lll} a_1^* = (1, \tau, 0) & a_2^* = (\tau, 0, 1) & a_3^* = (\tau, 0, -1) \\ a_4^* = (0, 1, -\tau) & a_5^* = (-1, \tau, 0) & a_6^* = (0, 1, \tau) \end{array}$$

Consequences are manifold:

- it is confirmed that the point symmetry is incompatible with periodic translational order in 3-dimension
- the G vectors do not define a reciprocal lattice but generate a set of points that fill the space densely
- the diffraction pattern is selfsimilar since τnG belongs to the set define by Eq. (3) or (4), given a vector G of this set
- and, last but not least, there is a periodic image of the quasiperiodic structure in a higher dimensional space. Indeed, Eq. (2) and (3) are formally equivalent. If Eq. (2) is used to define a 3-dim reciprocal lattice for a crystal structure, Eq. (3) can be used as well to define a 6-dim reciprocal lattice for a quasicrystal structure

(or other high-dim image for other symmetries than icosahedral). Let us call $R_{3//}^*$ the space containing the 3-dim G vectors and R_6^* such a 6-dim space containing a lattice of basic vectors e_i^* which project on a_i^* into $R_{3//}^*$. Then the vectors $\mathcal{G} = \sum_{i=1}^6 n_i e_i^*$ span this 6-dim lattice when the $G = \sum_{i=1}^6 n_i a_i$ span the $R_{3//}^*$; each \mathcal{G} project into $R_{3//}^*$ on one and only one G vector.

To the dense distribution of G vectors in $R_{3//}^*$ corresponds a density distribution ρ_3 in a direct space $R_{3//}$ which is dual of $R_{3//}^*$, via the Eq. (1). $R_{3//}$ is our physical space and ρ_3 is the structure of the quasicrystal of interest. Similarly, to the periodic reciprocal lattice \mathcal{G} in R_6^* corresponds a direct periodic lattice bearing a density distribution ρ_6 in a direct space R_6 , which is dual of R_6^* . The density distribution ρ_6 can be dubbed as the periodic image of the quasicrystal structure ρ_3 . Mathematics tell us that if distributions in two different spaces are related via projection, the Fourier transformed distributions in the dual associated spaces relate via a cut procedure. The correspondence scheme can then be summarised as follow:

$$\begin{array}{ccccc}
 & \rho_6(r) & \xleftrightarrow{FT} & F(\mathcal{G}) & \\
 \text{cut of } R_6 & \downarrow & & \downarrow & \text{Projection of } R_6^* \\
 \text{by } R_{3//} & \rho_3(r_{//}) & \xleftrightarrow{FT} & f(\mathcal{G}) & \text{onto } R_{3//}^*
 \end{array}$$

in which FT means of course Fourier transform and $r_{//}$ is the components in R_3 of the 6-dim vector r .

Using the high-dimensional image is a very efficient and economical way to describe a quasicrystal. We are thus back to normal crystallography in which one needs only to know a unit cell and a metric to design the whole structure. Moreover, this gives the easy way to operate diffraction experiment for structure determination: the diffraction peaks are indexed with six Miller indices according to Eq. (3) or (4) and then “lifted” into R_6^* formally to produce $F(\mathcal{G})$ whose Fourier transform gives $\rho_6(r)$; a final cut of $\rho_6(r)$ by our 3-dim physical space generate the quasiperiodic structure $\rho_3(r_{//})$.

It is, however, useful to describe in somewhat more details both the “Bravais” lattice and the unit cell motive of the periodic image $\rho_6(r)$. It is first of common use to refer to the physical space $R_{3//}$ as the parallel space or the internal space; the 3-dim space that must be added to $R_{3//}$ in order to complete R_6 is dubbed complementary space, or perpendicular space (hence $R_{3\perp}$ with its dual $R_{3\perp}^*$)

or external space. Each basis vector e_i^* of the reciprocal lattice in R_6^* projects on one $e_{i//}^* = a_i^*$ and on one $e_{i\perp}^*$ into $R_{3//}^*$ and $R_{3\perp}^*$ respectively. The scheme which relates the quasiperiodic structure to its periodic image imposes that at any symmetry operation in $R_{3//}^*$ correspond associated symmetry operations in $R_{3\perp}^*$ and R_6^* ; in other words the reciprocal lattice in R_6^* is invariant in any operation which preserve $e_{i//}^*$ and $e_{i\perp}^*$. Thus the six fivefold planes ($e_{i//}^*, e_{i\perp}^*$) are mirror planes of the 6-dim reciprocal lattice which, hence, is cubic and so is the direct lattice in R_6 (an N -cube has N mirror planes perpendicular to the rotational axes of the highest order). There are also ten threefold and fifteen twofold mirror planes. It is said that the point group of the lattice in R_6 is isomorphic to the icosahedral point group. The subspaces $R_{3//}$ and $R_{3\perp}$ have the same symmetries.

Now what does the density distribution $\rho_6(r)$ in this cubic lattice look like? First of all, the cut of $\rho_6(r)$ by $R_{3//}$ must generate a set of points that will accept atom positions. Thus, $\rho_6(r)$ must have no thickness in $R_{3//}$, i.e., must be a distribution of objects being "flat" in $R_{3//}$ or, in other words, completely located into $R_{3\perp}$. Let us call $A_{3\perp}$ these 3-dim objects which have been commonly named **Atomic Surfaces (AS)**. The main requisite to design the $A_{3\perp}$ are the following:

- they must be 3-dim polyhedra having symmetries of an icosahedron.
- they must obey a so-called hard core condition which constrains their size and shape so that cutting by $R_{3//}$ does not generate unphysically too short atom pair distances.
- they must allow energy translational invariance of the quasiperiodic structure parallel to both $R_{3//}$ and $R_{3\perp}$ spaces. Flatness in $R_{3//}$ guarantees translation invariance in this subspace. Translation invariance in $R_{3\perp}$ means that the $A_{3\perp}$ must form subset in which piecewise connection prevents annihilation/ creation of atoms under any $R_{3\perp}$ translation, while structures with differences into their detailed geometry may be generated. This is called the closeness condition [13].
- density and composition of the quasicrystal also operate on size, shape and partitioning of the atomic surfaces.

The simplest shape that may be attributed to the $A_{3\perp}$ volumes is spherical. But reducing the $A_{3\perp}$ objects of the high-dim image to their spherical approximation is obviously accepting a low resolution description of the structure. Here, the expression "low resolution" means that in the Fourier transform of the $A_{3\perp}$ atomic

surfaces the high-order Fourier components are not really accounted for. Sphere sizes are mostly fixed by density and composition constraints.

One possible method of introducing the high-order Fourier components is to parametrize the atomic surfaces in terms of linear combinations of symmetry-adapted functions associated with their point group symmetry [14]. In the case of an icosahedral quasicrystal, the perpendicular space is three-dimensional. The *spherical harmonics* are then a natural choice for expressing the boundaries of any radial functions $r(\theta, \phi)$. Hence the set of symmetry-adapted orthonormalized functions, invariant for icosahedral point group symmetry, can be chosen according to the decomposition

$$r(\theta, \phi) = \sum_{li} a_{li} Z_{li}(\theta, \phi) \quad (5)$$

with

$$Z_{li}(\theta, \phi) = \sum_m Z_{lm}(i) Y_{lm}(\theta, \phi)$$

in which Y_{lm} are the classical spherical harmonics, Z_{lm} are determined by the point group symmetry of the $A_{3\perp}$ plus the normalization conditions of Z_{li} , and a_{li} are continuous parameters to be fitted in structural diffraction analysis: the index i allows for the possible existence of several orthogonal invariant functions within the same subspace of functions having a given value of l .

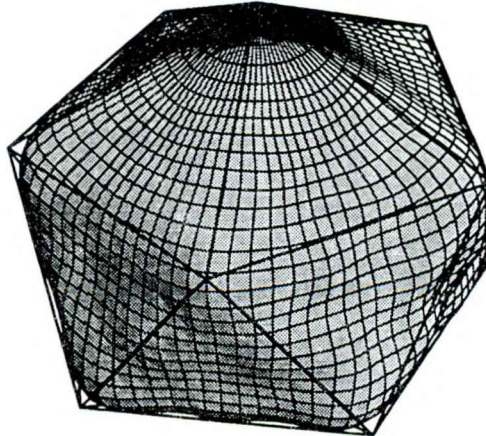


Figure 11: Approximation of an icosahedron by four spherical harmonics.

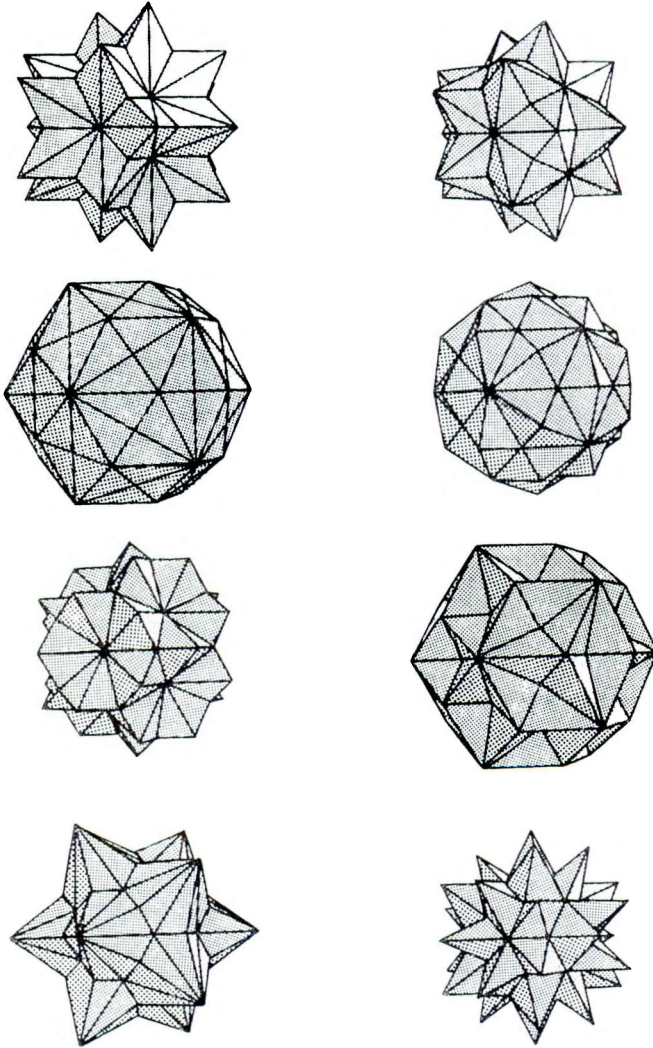


Figure 12: The eight basic polyhedra bounded by 2-fold planes in $R_{3\perp}$ for the 6-dimensional image structure of icosahedral quasicrystals [13].

If the point group is large enough, there will be many empty subspaces. For instance, with the icosahedral point groups there is a single invariant function (for l up to 15) only for l values of 0, 6, 10 and 12. Beyond $l = 15$, contributions to Eq. (5) are expected to be very weak. As an illustration, Figure 10 shows that these four components are sufficient for the reconstruction of an icosahedron certainly beyond experimental resolution. Any physical constraint on the $A_{3\perp}$,

such as those induced by realistic atomic distances, density, composition, etc., can be introduced in the refinement via penalty functions. This is probably a good basis for allowing successful least-squares refinement processes to obtain realistic faceted $A_{3\perp}$ objects.

The hard-core and closeness conditions mentioned above are satisfied if the $A_{3\perp}$ objects are bounded by piecewise connected surfaces, mostly parallel to the complementary space, without overlapping in this space, and globally invariant under point group symmetries. These conditions are satisfied for surface boundaries which are mirror planes of the structures. As a consequence, possible faceted $A_{3\perp}$ volumes for the 6-dim images of icosahedral quasicrystals would have 2-fold, 3-fold, or 5-fold plane boundaries. This point has been demonstrated in detail for 2-fold plane boundaries, [13] and the shapes of the eight corresponding polyhedra are presented in Figure 12. The acceptable volumes for decorating the 6-dim cube must be one of these polyhedra, or any τ -scaling and/or intersection of them. Obviously, this leaves a number of alternative solutions and the formal faceting conditions, as they stand, have to be considered mostly as a negative test to reject improper solutions.

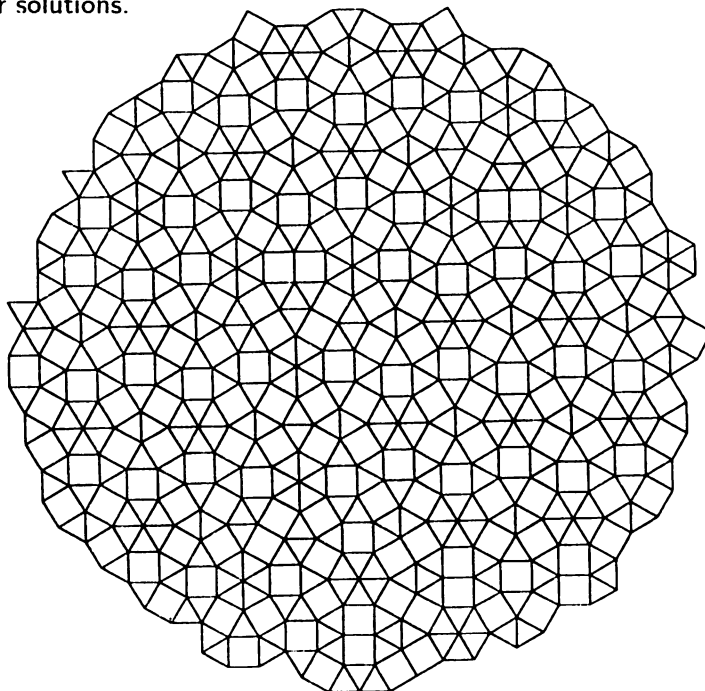


Figure 13: Finite portion of a dodecagonal planar quasicrystal with square- triangle prototiles [15].

So far we have assumed that the $A_{3\perp}$ atomic objects of the high-dim image are (faceted) polyhedra. This has induced conditions for these atomic objects. It may be of interest to consider whether the polyhedral solution is imposed in every case. There is no general answer to this question, and the point has received very little investigation, with restriction to 1-dim and some 2-dim quasiperiodic structures. One example has been reported by Baake et al. [15]. They generated a quasiperiodic dodecagonal tiling of the plane using squares and regular triangles arranged with simple deflation-inflation symmetries (Fig. 13). This 2-dim structure has been “lifted” (embedded) into a 4-dim periodic lattice and the acceptance domain (or A_{\perp} objects) has been iteratively constructed to generate the vertex set of the square-triangle tiling. The result is shown in Figure 14. The procedure leads to a fractally bounded A_{\perp} . It can be shown that there is no polyhedral alternative solution if the square-triangle tiling is to be obtained with a single type of A_{\perp} .

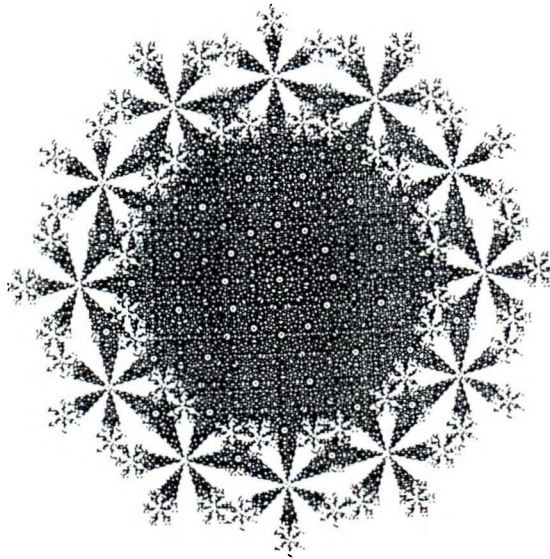


Figure 14: Acceptance domain in R_{\perp} filled by lifting 32000 vertices of the tiling shown in Figure 13 [15].

The hyperspace image of the Fibonacci chain

As a quasiperiodic 1-dim structure requires at least two different segments for avoiding periodicity, the corresponding periodic image is at least two-dimensional. In the absence of 1-dim point group, this 2-dim Bravais lattice may be any of

the five existing ones. A square lattice may be the best choice for the sake of geometrical simplicity and also for mimicking at best the 6-dim cubic lattices that correspond to icosahedral real quasicrystals. The atomic surfaces A_{\perp} must be "flat" in the direction R_{\perp} which is perpendicular to the direction $R_{//}$ of the chain. Hence, they are simple straight line pieces with the length Δ , as shown in Figure 15. The position of $R_{//}$ (and then R_{\perp}) in R_2 is fixed by the angle α of $R_{//}$ with respect to the horizontal raw of the square lattice. If $\tan \alpha$ is an irrational number, the structure of the chain is aperiodic, with two different tiles $L = a \cos \alpha$ and $S = a \sin \alpha$. The closeness condition is fulfilled provided that

$$\Delta = a(\cos \alpha + \sin \alpha)$$

The average density of the chain must be transferred to its image and, hence, is equal to $\Delta/a^2 = (\cos \alpha + \sin \alpha)/a$. Finally, L/S being equal to τ in a Fibonacci chain fixes the angle α and there is no free parameter left for the periodic image.

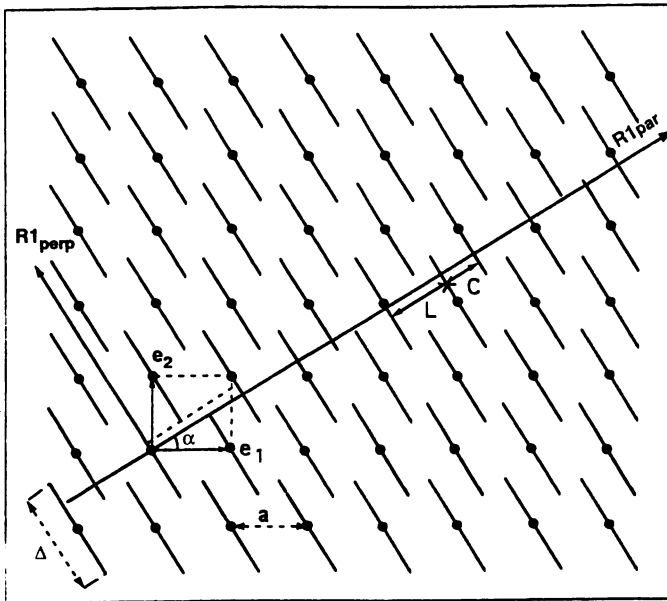


Figure 15: Toy-model of the hyperspace image for a quasicrystal. Here is shown a 1-dimensional Fibonacci chain and its 2-dimensional periodic image as a decorated square lattice.

Moving the $R_{//}$ direction across the decorated square lattice generates all the equiprobable structures with the same energy but differing locally in their geom-

etry features. All these isomorphic structures relate to each other via “atomic jumps”, so-called phason-jump, due to flipping in $L - S$ sequences (see Fig. 15).

The physical generation of quasiperiodic patterns may be very simple

Detailed description of the atomic surfaces using diffraction data with real quasicrystals is very difficult, may be impossible to be achieved and, so far, only low resolution structures have been obtained. But the main drawbacks of the high dimensional scheme are twofold: (i) the crude resulting physical structure in the three-dimensional space is concealed in a list of atomic positions without any clear guides on how to design straightforwardly space occupation and, even more disturbing, (ii) there is a total lack of how to grow the whole structure by adding atomic positions one by one or, to the least, cluster by cluster.

Actually, growing a piece of matter within certain rules for short and long range order is not an easy task. For regular periodic crystals, the sequence of atoms that exists in a seed cluster repeats exactly again and again; so it appears that the atom to be added must interact only with a small number of atoms at some places on the cluster surface. Moreover, there is a single ground state structure for a given space group which means that the structure is energetically stabilised and can be grown perfectly. The various mathematical procedures that have been used so far to generate quasiperiodic lattices are somewhat suggestive that growing a perfect quasicrystal would be a daunting task. The sequence of atoms never exactly repeats, so that atoms added to the surface of a cluster must interact with each atom in the seed cluster to ensure that it sticks at a site consistent with perfect quasiperiodic order. As the cluster grows, this requirement imposes arbitrary long-range interaction, which is physically implausible. Matching rules, particularly well exemplified with the Penrose tiling, would then seem to offer a potential mitigating factor to these growth problems. The classical edge-matching rules are typically indicated by placing different arrows on the edges of tiles that constrain the way two tiles must match edge-to-edge. Penrose clearly showed that the only plane-filling tiling consistent with the matching rules is a perfect Penrose tiling. Do these edge-matching rules also represent viable local rules for growing a tiling by adding one tile at a time to a random chosen edge? Unfortunately not. Mistakes are made which are not revealed at once and the catastrophe can be appreciated only after many further building steps. Removing tiles for another or other tries is obviously a dismal failure of the

edge-matching rules as a growth procedure [16]. Replacing edge-matching rules by “forced vertex-matching rules” has certainly relaxed part of the difficulties but the basic drawbacks remain the same [17]. Recently, Moody and Patera [18] have described a mathematical procedure to grow quasiperiodic structures via strictly local rules in which a point is added to the growing patch if and only if (i) an ideal configuration is not violated and (ii) the point phase in the physical space remains within a chosen range of values. But, still, local phases are correlated to each other and are not exactly direct space parameters. However, it is possible to keep the spirit of the method and derive a purely local growth procedure that, moreover, is consistent with structure and properties of real quasicrystals.

Among the many properties of quasicrystals observed so far, two of them deserve to be selected for the present purpose: (i) their structure appears as basically built from packing of very rigid atomic clusters with “forbidden” symmetries and (ii) their shear modulus [19] is as large as those obtained with semiconductors revealing strong directional atomic bonding. One very simple way to preserve what can be preserved of that while growing the structure is to proceed as follows [20]:

- (i) A “star” of atomic bonding is deduced from a given cluster of atoms. In the two-dimensional example of a decagonal centred cluster (Fig. 16(a)), the “star” is made of the ten radial vectors linking centre to vertices and dispatched at $2\pi/10$ angles from each other (cluster requisite).
- (ii) The above “star” of vectors defines the only possible translations, originating from an existing site at the surface of the growing structure, to create new sites (directional bonding requisite).
- (iii) New sites that would introduce too short pair distances, with respect to the already existing sites, are rejected (finite density requisite). The point is illustrated with Figures 16(b) and 16(c) which show a second growing step from a decagonal cluster and what is preserved if too close positions are erased; in this example, the threshold pair distance has been fixed to the length of the decagonal edges. Figure 17 shows a piece of one structure that can be iteratively generated by pursuing again and again the above addition procedure with the same decagonal star.

That this procedure is easily feasible and allows structure growth via purely single local rules is then now obvious. It remains that at least two basic questions

must be carefully addressed: (i) does this mechanism generate a single state structure or, conversely, a variety of “energetically” equivalent structures and (ii) does it truly result into quasiperiodicity.

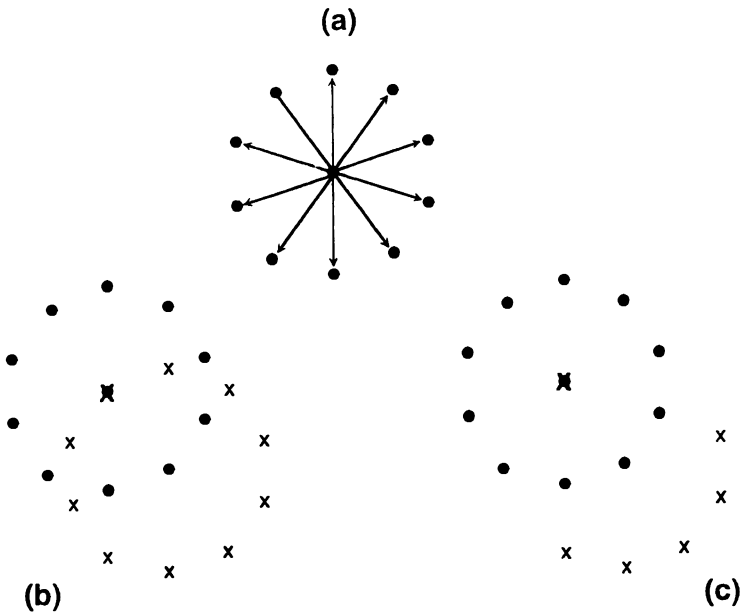


Figure 16: (a) Decagonal cluster of sites defining a ten-fold star of vectors; (b) A second decagon of sites (•) has been added to the one shown in (a), with its centre on a vertex site; (c) same as in (b) except that sites overly close to those of (a) are removed.

If combinations of two-, three-, four and six-fold stars of vectors are used in the growing sequence, one gets trivially lattices of sites which are periodic crystal lattices and it has been well known for almost a century that one given star generates one and only one lattice. With pentagonal, decagonal, icosahedral ... stars it is not possible any more to generate lattices and fully dense set of sites are obtained instead, if there is no restriction made on pair distances. The physical constraint on density via the rejection rule of too close atoms is then usefully applied. But, clearly, which particular new sites have to be rejected strongly depends on which sites are already there, which in turn depends on the order chosen to explore the surface sites of the growing structure. This exploration can be made at random which gives prospects for an infinite number of very slightly

different structures (Fig. 18); or else one may decide to circle the seed always in, say, a step by step clockwise exploration of the surface sites, which generate the more regular structure of the family with an overall symmetry axis in its centre. Conclusively, the procedure does not generate a single state structure but, rather, a family of very similar packing of sites.

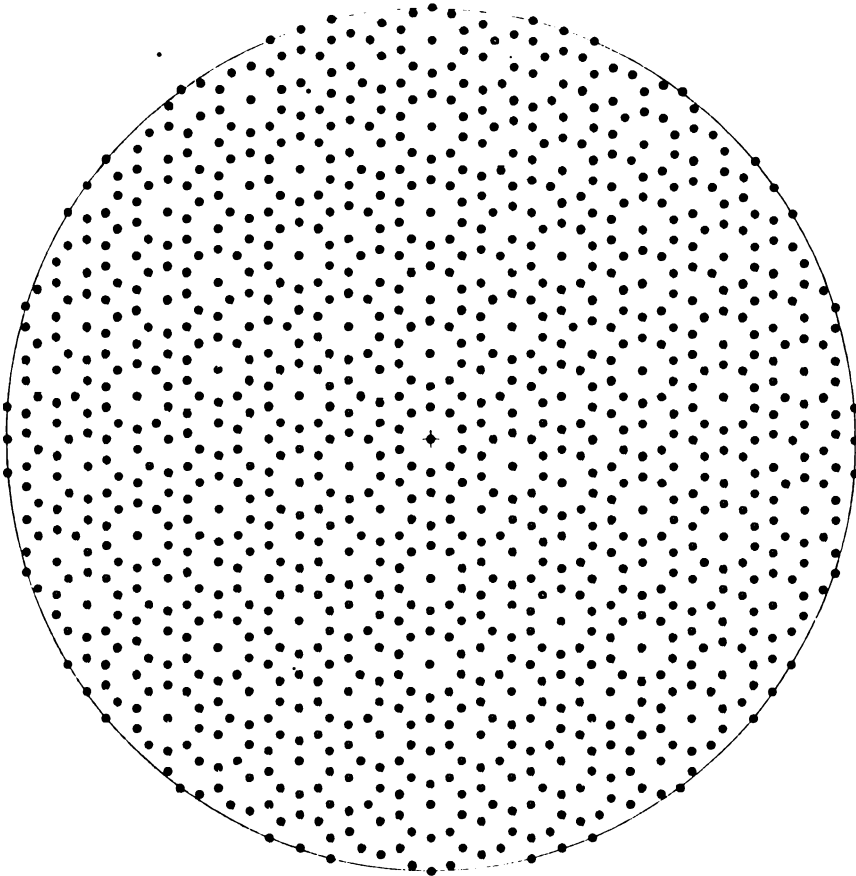


Figure 17: A piece of structure grown using a tenfold star and shortest distances slightly below the edge length of the decagon.

The question of true quasiperiodicity of the obtained structures is less easily overcome even if encouraging insight can be proposed. Of course, the trivial requisite is that vector stars that generate crystal lattices must be strictly avoided. This being said, the geometrical scheme described here is more related to the hyperspace description than it would seem at first sight. Indeed, specifying the high dimensional Bravais lattice by its translation vectors corresponds to the se-

lection of a star of vectors in the three-dimensional physical space. Adding to this hyperlattice some atomic surfaces is equivalent to define acceptance domains for permitted atomic pair distances and directions. Thus, our growing scheme exhibits the two main ingredients that should allow to generate quasiperiodic structure. As a positive illustration of this statement, Figure 19 presents an impressive comparison between a structure obtained via the “star-short distance” scheme (*SSDS*), the one already shown in Figure 2 actually and, on the other hand, a five-fold planar cut of an atomic arrangement deduced from diffraction data with an AlPdMn real quasicrystal via the hyperspace method and within spherical approximations for the atomic surfaces. This is a strong support to the double suitability of the procedure to generate structures that can be quasiperiodically ordered and even describe real quasicrystal quite nicely. But it seems that the conclusion is not universal whatsoever. A contradictory example is given in Figure 20 which shows a structure grown with a pentagonal star and short-distance threshold equal to the pentagon radius; this is obviously nothing else than a pentatwinned regular crystal. This is actually not deeply surprising and may be related to the well known possibility to generate either quasicrystals or some sorts of twinned crystals via the hyperspace scheme. At this stage we cannot refrain from thinking that, finally, quasicrystals are less difficult to describe than suggested so far and, also, that they can be grown via the simplest mechanism, i.e. adding one atom at a time.

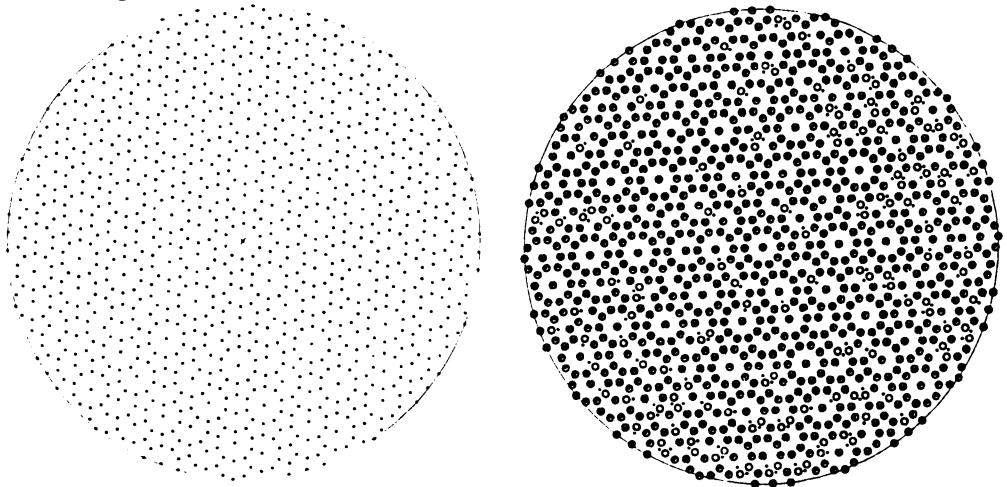


Figure 18: (a) Same conditions as in Figure 2 but with another random exploration of the surface sites; (b) Figure 17 and 18(a) have been superimposed. Solid dots appear whenever the two structures coincide.

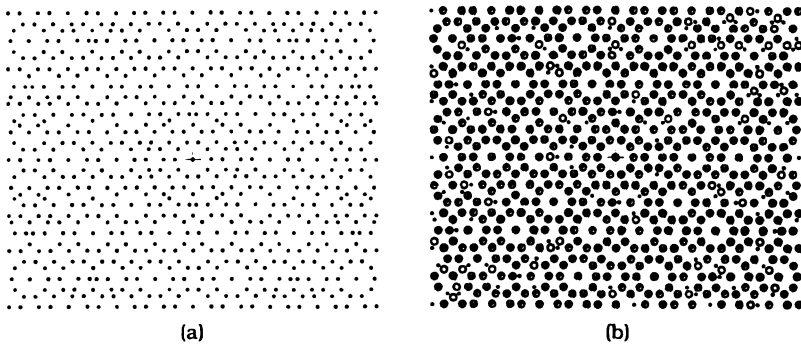


Figure 19: (a) One planar cut of the structure of a real quasicrystal; (b) Figure 17 and 19(a) have been superimposed. The overlap is quite impressive [20].

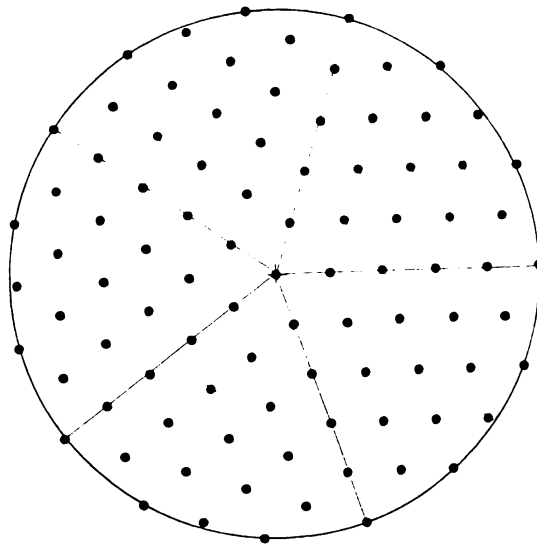


Figure 20: The structure grown with a five-fold star and shortest distance equal to the radius of the pentagon is a pentatwinned crystals.

A few more words about the geometry of real quasicrystals

The structure of real quasicrystals is generally obtained from diffraction data via the hyperspace approach to their periodic images. As already said, one must unfortunately be contented with rather low resolution structure, due to the poor definition of the atomic surfaces actually reached. However, clear building rules

are revealed, with evidences of both geometrical and chemical order. The point is going to be exemplified with the structure of AlPdMn quasicrystals which offer the rare privilege to be growable as centimetre size single grain [21].

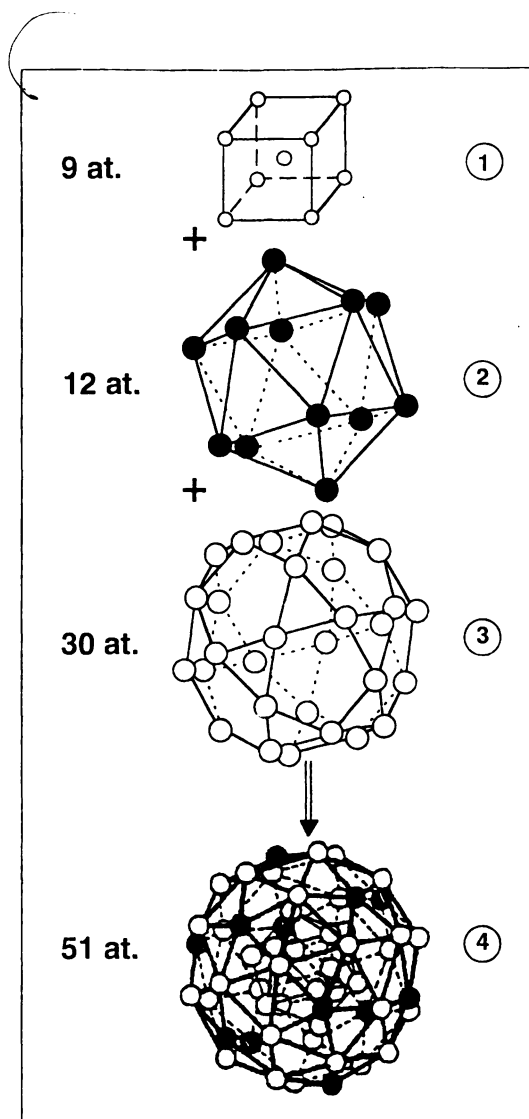


Figure 21: Successive atomic shells of a pseudo-Mackay icosahedron (PMI).

First of all, everything in the structure is based on atomic units containing 51 atoms in total, named pseudo-Mackay icosahedra (PMI) hereafter, and made of three centrosymmetrical shells as shown in Figure 21: an inner small centred

cubic core of 9 atoms, an intermediate icosahedron of 12 atoms, and an external icosidodecahedron of 30 atoms. The last two shells have practically equal radii and constitute altogether the boundary of the PMI whose diameter is slightly less than 10 \AA . Apart from this well-defined geometry, the PMI's show three different chemical compositions: one family (PMI-A) has 6 manganese plus 7 palladium atoms on the icosahedron and centre sites and 38 aluminium atoms elsewhere while the two other families (PMI-T) exhibits 20 or 21 palladium atoms among the 30 of the icosidodecahedron, the rest (30 or 31 atoms) being aluminium atoms. The calculated atomic density of an individual PMI is $0.064 \text{ atoms/\AA}^3$, which compares quite well with the measured density of the bulk material, within experimental accuracy. It is, however, fair to say that several ingredients in the description of the PMI's do not show up directly from diffraction data. The Patterson analysis strongly suggests that the PMI cores are made of about 8-9 atoms distributed into pieces of dodecahedra; it is indeed a speculation to state that these pieces are arranged in centred cubic geometry. It is probably better to consider that we have a dodecahedral core whose 20 sites are only partially occupied.

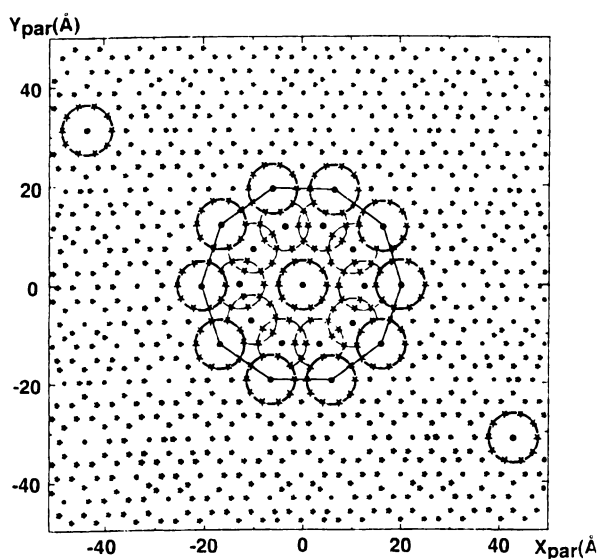


Figure 22: Fivefold planar cut of the structure of the AlPdMn quasicrystal. Rings of ten atoms are equatorial section of a PMI. The τ^3 and τ^2 -inflated rings are visible [21].

Then, these PMI units combine to reproduce a selfsimilar geometry within inflation by a scale factor close to τ^3 . This is shown in Figure 22 which presents

the cut of a piece of the structure by a plane perpendicular to a fivefold axis. In the figure centre, the equatorial section of a PMI shows up. Around this central PMI, there are 42 PMI's whose centres are distributed on the combined sites of the icosahedron plus the icosidodecahedron of a big PMI with a radius τ^3 as large as that of the base unit (about 42 Å, namely). An intermediate shell, with τ^2 inflated radius, is also visible in Figure 22. This shell is made of overlapping PMI's and is the inflated modification of the partially occupied dodecahedral core of the basis PMI unit. The overlapping is such that preservation of the density is ensured, within very low residual fractality.

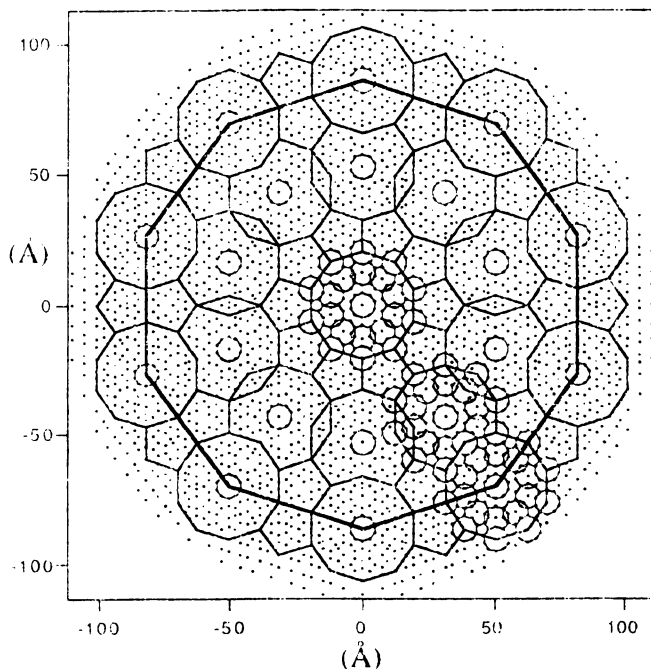


Figure 23: Same as in Figure 22 but with an additional inflation step of the structure.

The structure subsequently develops via successive steps of τ^3 inflation operations. Figure 23 shows a planar projection of a layer of atoms presenting the result of a $\tau^3 \times \tau^3$ inflation, with a τ^3 -PMI in the centre, a shell of 42 τ^3 -PMI on a $\tau^3 \times \tau^3$ radius "sphere" and the $\tau^3 \times \tau^2$ intermediate shell of overlapping truncated τ^3 -PMI. Pentagonal "tiles" at various scales are also visible in the figure; they come from PMI and inflated PMI whose equatorial plane is not in the figure. In conclusion, at any inflation stage, we have a cluster of PMI clusters.

The Figures 19(a) and 23 are actually slightly different representations of the same data which, at two different levels, demonstrate the leading aspect of the basic cluster stability into natural growth of quasiperiodicity. It has been also observed that the selfsimilarity rules that describe the geometry also apply to the chemistry of quasicrystals [21].

References

- [1] Senechal M., *The geometry of quasicrystals*, (Cambridge University Press) 1995; Janot C., *Quasicrystals: a primer* (Oxford University Press, Cambridge) 2nd edition 1994.
- [2] Tsai A. P., Inoue A. and Masumoto T., *Phil. Mag. Lett.* **62** (2) (1990) 95.
- [3] Kycia S. W., Goldman A.I., Lograsso T.A., Delaney D.W., Sutton M., Dufresne E., Bryning R. and Rodricks B., *Phys. Rev. B* **48** (1993) 3544.
- [4] Boudard M., Bourgeat-Lami E., de Boissieu M., Janot C., Durrand-Charre M., Klein H., Audier M. and Hennion B., *Phil. Mag. Lett.* **71** (1995) 11; Audier M. and Hennion B., Durand-Charre M. and de Boissieu M., *Phil. Mag. B* **68** (1993) 607.
- [5] Boudard M., de Boissieu M., Janot C., Heger G., Beeli C., Niessen H. U., Vincent H., Ibberson R., Audier M. and Dubois J. M., *J. Phys. Condens. Matter* **4** (1992) 10149.
- [6] Janot C., *Europhysics Letter* **27** (1996) 60.
- [7] Pierce F. S., Guo Q. and Poon S.J., *Phys. Rev. Lett.* **73** (1994) 2220 ; Guo Q. and Poon S.J., *Phys. Rev. Lett.* (in press).
- [8] Dzugutov M., *Phys. Rev. A* **46** (1992) R2984; *Phys. Rev. Lett.* **70** (1993) 2924; Quemerais P., *J. Phys. I* (France) **4** (1994) 1669.
- [9] Zurkirsh M., Atrei A., Erbudak M. and Hochstraser M., *Phil. Mag. Lett.* **73** (1996) 107; Ebert P., Feuerbacher M., Tamura N., Wollengarten M. and Urban K., *Phys. Rev. Lett.* **77** (1996) 3827.
- [10] Penrose R., *Bull. Inst. Math. Appl.* **10** (1974) 266.

- [11] Burkov S. E., *J. Phys. I (France)* **2** (1992) 695; Gummelt P., in *Quasicrystals* (Ed. C. Janot and R. Mosseri) World Scientific, Singapore (1995) p. 84; *Geometriae Dedicata* (in press).
- [12] Jeong H. C. and Steinhardt P. J., *Phys. Rev. Lett.* **73** (1994) 1943; Khanna S. N. and Jena P., *Phys. Rev. B* **51** (1995) 13705; Janot C. and de Boissieu M., *Phys. Rev. Lett.* **72** (1994) 1674.
- [13] Katz A. and Gratias D., *J. Non-Cryst. Solids* **153–154** (1993) 187; Katz A., in *Number Theory and Physics* (Ed. J.M. Luck, P. Moussa, W. Waldschmidt and C. Itzykson) Springer, Berlin (1990) p. 100; Katz A. and Gratias D., in *Quasicrystals* (Eds. C. Janot and R. Mosseri) World Scientific, Singapore (1995) p. 164.
- [14] El Coro L., Perez-Mato J.M. and Madariaga G., *J. Non-Cryst. Solids* **153–154** (1993) 155.
- [15] Baake M., Klitzing R. and Schlottman M., *Physica A* **1991** (1992) 554.
- [16] Penrose R., in *Introduction to the Mathematics of Quasicrystals* (Ed. M. Jaric) Academic Press, New York, 1989, p. 53; Gardner M., *Sci. Am.* **236** (1977) 110.
- [17] Onoda G. Y., Steinhardt P. J., Di Vincenzo D. P. and Socolar J. E. S., *Phys. Rev. Lett.* **60** (1988) 2653.
- [18] Moody R. V. and Patera J., *Lett. Math. Phys.* **36** (1996) 291.
- [19] Tanaka K., Mitarai Y. and Koiwa M., *Phil. Mag. A* **73** (1996) 1715.
- [20] Janot C. and Patera J., *Phys. Rev. Lett.* (submitted).
- [21] Janot C., *Phys. Rev. B* **53** (1996) 181; *J. Phys.: Condens. Matter* (submitted).